A&A 506, 677–680 (2009)
DOI: 10.1051/0004-6361/200911774

Astronomy & Astrophysics

HI-observations of dwarf galaxies in the Local Supercluster⋆ *(Research Note)*

W. K. Huchtmeier[1], I. D. Karachentsev[2], and V. E. Karachentseva[3]

[1] Max-Planck-Institut für Radioastronomie, Auf dem Hügel 69, 53121 Bonn, Germany
e-mail: huchtmeier@mpifr-bonn.mpg.de
[2] Special Astrophysical Institute, Russian Academy of Sciences, N. Arkhyz, KChR, 369167, Russia
e-mail: ikar@luna.sao.ru
[3] Astronomical Observatory of Kiev University, Kiev, Ukraine
e-mail: vkarach@observ.univ.kiev.ua

Received 3 February 2009 / Accepted 29 June 2009

ABSTRACT

We have observed 71 dwarf galaxies of low surface brightness using the 100-m radio telescope at Effelsberg in a search for new members of 27 northern galaxy groups with characteristic distances of 8 to 15 Mpc. We present radial velocities, HI-fluxes, and HI line widths for 17 detected galaxies as well as upper limits for the remaining undetected objects. Almost all detected dwarf galaxies are physical members of the corresponding group with a mean radial velocity difference of -9 ± 45 km s^{-1} with respect to the principal galaxy in each group. Our sample of new dwarf members of nearby groups has a median radial velocity of 700 km s^{-1}, a mean blue absolute magnitude of –12.7 mag, a mean linear diameter of 2.5 kpc, and a mean $M_{\rm HI}/L_{\rm B}$ ratio of 1.1 $M_\odot/L_\odot$. The Ir galaxy d1217+4703 in the Canes Venatici I cloud turns out to be a very gas-rich galaxy with $M_{\rm HI}/L_{\rm B} = 6.5$ in solar units.

Key words. galaxies: dwarf – galaxies: evolution – galaxies: ISM

1. Introduction

In this paper, we present another step in the search for *new* dwarf galaxies in the nearby universe. Adding *new* dwarf galaxies makes it possible to study in more detail the galaxy luminosity function, the morphological segregation in groups, and the dependence of physical parameters of dwarf galaxies on their immediate environment. In addition, the improved membership information of groups will be helpful in analysing the kinematics and dynamics of galaxy groups.

Systematic all-sky searches of the POSS-II and ESO/SERC sky surveys for nearby dwarf galaxies (out to distances of ~6 Mpc) followed by 21-cm HI line observations doubled the number of known dwarf galaxies in the nearest galaxy groups (see "A catalog of neighbouring galaxies" by Karachentsev et al. 2004, and references therein). This was followed by another search for the galaxy dwarf population in the more distant Leo-I group (10.4 Mpc) Karachentsev & Karachentseva (2004). Thirty-six dwarf galaxy candidates have been found, and 21-cm HI line observations with the 305-m Arecibo radio telescope confirmed the group membership of most of them (Stierwalt et al. 2009). This positive result motivated us to extend the search for dwarf galaxies to other more distant groups. Karachentsev et al. (2007) presented a list of new dwarf galaxy candidates in 27 northern groups with distances in the range of 8 to 15 Mpc selected from the POSS-II sky survey. Within a total area of ~2000 square degrees, we found 90 low surface brightness objects of which 54 have not been catalogued so far. Several of these objects were observed in the 21-cm HI line with the Effelsberg 100-m radio telescope from 2004 to 2006. These observations confirmed that the detected galaxies belong to the dwarf population of these galaxy groups in terms of their radial velocity, luminosity, line width, and HI-content.

The survey presented here extends our previous search for HI-emission from nearby dwarf galaxies within distances of ~6 Mpc (Huchtmeier et al. 2000, 2001) and from dwarf galaxy candidates found in nearby groups (Karachentsev et al. 2007). We have added to our search list some dwarf galaxies recently found in both the Leo-I group and in the M81 group.

2. HI-observations

The HI observations were completed using the 100-m radiotelescope, which has a half power beam width of 9.3′ at a wavelength of 21 cm. The 1024-channel autocorrelator was devided into four filter banks (256 channels each) using a bandwidth of 6.25 MHz, which yielded a resolution of 6 km s^{-1} or 10 km s^{-1} after Hanning smoothing. In a second run in 2007, the old autocorrelator was replaced by the 8192-channel autocorrelator (AK90), which was devided into 4 filter banks of 2048 channels each, using a 10 MHz bandwidth. This yielded a resolution of about 1 km s^{-1} (but was broadened to ~10 km s^{-1} by applying a Gaussian filter). This frequency coverage corresponds to a coverage in radial velocity of 2600 or 2100 km s^{-1}, respectively.

A typical observing time of 60 min per source yielded a rms noise of ~4 mJy (the system noise was 30 K). Most of the observations were repeated to improve the signal-to-noise ratio and the reliability. An ON-source position was combined with an OFF-source position every 10 min. This total power mode improves the baseline stability of the spectra. Frequent measurements of well known continuum sources (e.g., 3C48, 3C147, 3C286, 3C353 (Ott et al. 1994) were used to control the pointing

⋆ Appendix and Table 3 are only available in electronic form at htpp://www.aanda.org

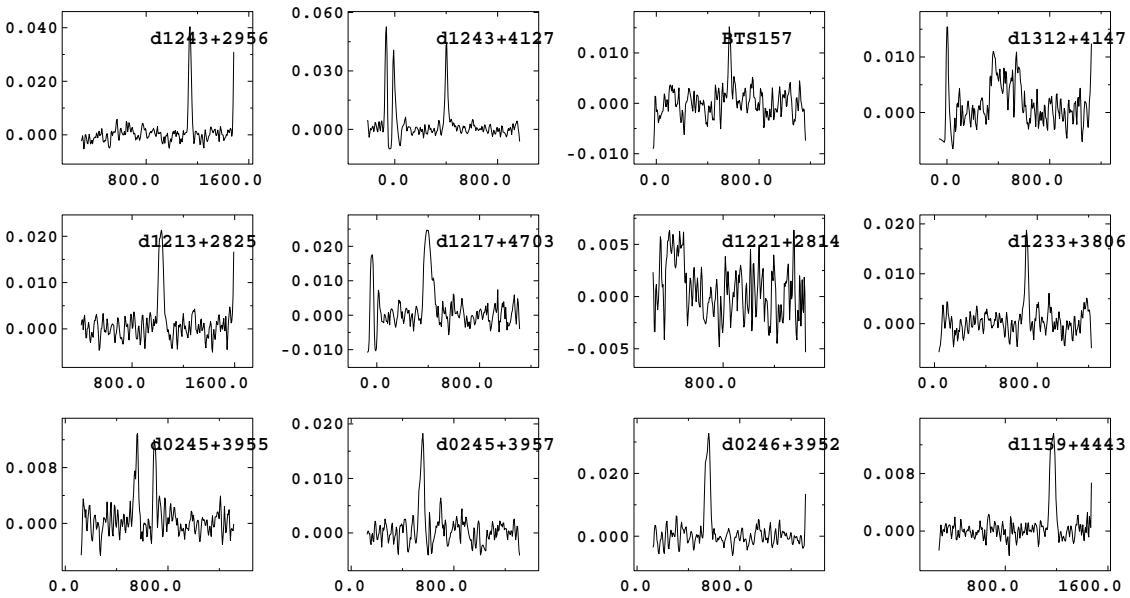

Fig. 1. a) HI profiles of the 12 dwarf galaxies detected in the Effelsberg observations from the first observational run with the AK1024, with a pencil beam of half-power beamwidth of 9.3 arcmin at 21-cm. All these galaxies have been detected for the first time. Profiles are arranged in an increasing order of right ascension, starting at the bottom left corner. (see Table 1). The axes are labelled in Jansky (Jy) and in heliocentric radial velocity in km s^{-1}.

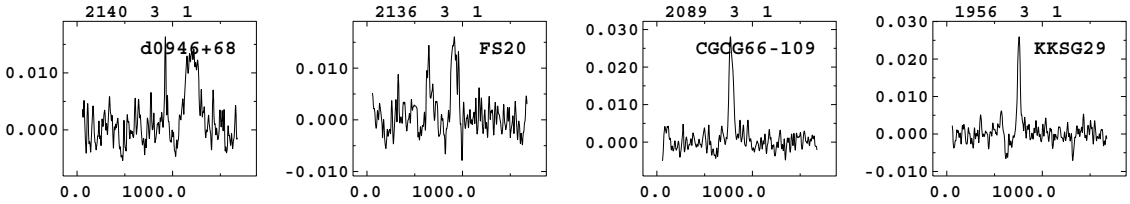

Fig. 1. b) HI-profiles from the second run in 2007 using the 8192-channel autocorrelator (AK90).

and calibration of the telescope. Every two to three hours, a well known line source (e.g., Holmberg I, DDO216, DDO221, Tifft & Huchtmeier 1990) was observed as a system check. These particular dwarf galaxies were selected because of their small line widths; the measured line parameters are relatively insensitive to baseline corrections. The *toolbox* software of the MPIfR was used for the data reduction. The observed spectra were corrected for moderately curved baselines (of second or third order) only; this should not introduce additional errors in the estimated velocities and flux densities of the lines since the line profiles are quite narrow in nearly all cases.

From the observed 71 dwarf galaxies, 17 were detected in HI (see Fig. 1). This detection rate of ∼24% is markedly lower than ∼79% found for our sample reported in Huchtmeier et al. (2005). The difference is probably caused by the ∼2 times higher average redshift of the present sample. Another reason, caused by the greater distances of the present sample galaxies is the reduced angular separation from more massive galaxies, which resulted in more cases of confusion. The greatest influence on the non-detection, however, is the increased activity of radio frequency interference within the protected band at 21-cm wavelength which blanked certain frequency ranges and produced some slowly varying spectral features in other cases. RFI was often observed in the velocity ranges 600 ± 10 km s^{-1}, 970 ± 20, 3500 to 4000, and 4300 to 4400 km s^{-1}. Only by repeating all observations several times, could we differentiate RFI and HI-emission in some cases. The receiver was tuned to the frequency corresponding to the group velocity (group membership as given in Table 3.

Table 1 summarizes the observational data: the galaxy name in Col. 1; coordinates (J2000) in Col. 2, as used for the observations; the optical dimensions in arcmin estimated by eye on the POSS-II corresponding approximately to the blue surface brightness level at ∼26.5 mag arcsec^{-2} (Holmberg level) in Col. 3; the blue apparent magnitude estimated bye eye on the POSS-II in Col. 4 with an estimated error of ∼0.5 mag (e.g., Sharina et al. 2008); the morphological type (T) estimated on the POSS-II in Col. 5; the optical heliocenctric radial velocity and its error in km^{-1} according to the SDSS DR4[1] in Col. 6. The HI data follow, i.e., the measured HI flux and its error according to Schneider et al. (1990) as follows:

$$\sigma_{\mathrm{HI-flux}} = 2(1.2W_{20}/v_{\mathrm{r}})^{0.5} v_{\mathrm{r}} {\sigma_{\mathrm{rms}}}^{2}$$

where v_{r} is the velocity resolution, σ_{rms} is the rms noise, the line width W_{20} has been replaced by 1.1 W_{50} (this relation is the average from 20 galaxies with appropriate signal-to-noise ratio) (Col. 7), the observed peak flux of the line and its rms error in Col. 8, the heliocentric radial velocity derived from the midpoint of the line at 50% of the peak and its error (Col. 9), and the linewidth at a level of 50% of the line peak (W_{50}) and, whenever clearly above the noise, the 25% level (Col. 10).

The derived global parameters for non confused objects in our sample of galaxies are presented in Table 2, the galaxy

[1] http://www.sdss.org/DR4

[2] The factor of two has been added to account for uncertainties in the baseline. However, for the narrow lines of dwarf galaxies, this yields an overestimation of the error.

Table 1. Observational data.

Galaxy name	RA, Dec (2000) h m s ° ′ ″	Optical size [arcmin]	m_B	T	Opt. vel. [km s^{-1}]	HI-flux [Jy]. [km s^{-1}]	HI-Peak flux [mJy]	H I velocity [km s^{-1}]	H I linewidth [km s^{-1}]
d0245+3955	02 45 30.8 +39 55 47	0.35 × 0.30	18.1	Ir		0.4 ± 0.07	12 ± 2	697 ± 6	26 31
d0245+3957	02 45 50.7 +39 57 11	0.90 × 0.75	16.8	Ir		1.0 ± 0.08	19 ± 2	552 ± 7	31 51
d0246+3952	02 46 00.6 +39 52 38	0.70 × 0.50	17.0	Ir		1.5 ± 0.10	35 ± 2	550 ± 4	44 55
d0946+6842	09 46 13.8 +68 42 55	0.15 × 0.15	20.5	Ir		1.6 ± 0.51	17 ± 5	1187 ± 3	184
FS 20	10 46 54.8 +12 47 17	0.40 × 0.30	18.2	Ir		1.4 ± 0.33	30 ± 5	928 ± 4	81
LeG 18		0.80 × 0.60	18.0	Ir		0.6 ± 0.25	23 ± 5	667 ± 4	50
CGCG66-109	11 04 26.5 +11 45 18	0.90 × 0.35	16.2	Ir	982 ± 78	1.6 ± 0.15	31 ± 3	779 ± 3	49 62
d1159+4443	11 59 59.2 +44 43 04	0.70 × 0.50	17.1	Ir		0.6 ± 0.10	16 ± 2	1168 ± 5	46 55
d1213+2825	12 13 19.1 +28 25 18	0.90 × 0.60	17.4	Ir	1020 ± 30	0.9 ± 0.19	22 ± 4	1026 ± 5	43 54
d1217+4703	12 17 10.1 +47 03 49	0.35 × 0.25	18.5	Ir		1.7 ± 0.28	25 ± 5	394 ± 5	61 95
d1221+2814	12 21 58.4 +28 14 34	0.60 × 0.45	17.8	Ir		0.7 ± 0.39	11 ± 4	450 ± 8	186 193
d1233+3806	12 33 07.4 +38 06 58	0.50 × 0.40	17.5	Ir		0.6 ± 0.10	21 ± 3	719 ± 4	23 39
KKSG29	12 37 14.1 –10 29 51	1.10 × 0.60	16.54	Im		1.0 ± 0.16	35 ± 4	756 ± 2	30 36
d1243+2956	12 43 44.2 +29 56 03	0.60 × 0.40	17.5	Ir		1.0 ± 0.14	44 ± 4	1141 ± 3	22 30
d1243+4127	12 43 55.7 +41 27 25	1.40 × 0.60	17.2	Ir		1.2 ± 0.12	51 ± 4	402 ± 2	16 26
BTS157	12 51 14.5 +47 04 06	0.70 × 0.50	17.5	Ir		0.5 ± 0.12	20 ± 4	572 ± 4	18 26
d1312+4147	13 12 58.7 +41 47 12	1.20 × 0.80	16.4	Ir	529 ± 40	1.5 ± 0.55	14 ± 5	460 ± 5	234 250

Table 2. Derived parameters for the detected galaxies.

Galaxy name	V_{LG} [km s^{-1}]	Dist. D Mpc	Diam. $A_{0,i}$ kpc	Abs. mag. M_B	H I mass [10^8 $M_\odot$]	L_B [10^8 $L_\odot$]	M_{HI}/L_B [$M_\odot/L_\odot$]
d0245+3955	886	12.1	1.2	–12.7	0.14 ± 0.02	0.17	0.82
d0245+3957	741	10.2	2.7	–13.6	0.24 ± 0.02	0.40	0.6
d0246+3952	739	10.1	2.1	–13.4	0.36 ± 0.02	0.32	1.12
d0946+6842	1327	18.2	0.8	–11.2	1.24 ± 0.39	0.04	31
FS20=LeG19	780	10.7	1.2	–12.1	0.38 ± 0.08	0.10	4.0
LeG18	519	7.1	1.6	–11.4	0.07 ± 0.03	0.05	1.4
CGCG66-109	631	8.6	2.2	–13.6	0.28 ± 0.03	0.37	0.76
d1159+4443	1207	16.5	3.4	–14.0	0.38 ± 0.06	0.59	0.64
d1213+2825	989	13.5	3.5	–13.3	0.39 ± 0.09	0.32	1.22
d1217+4703	452	6.2	0.6	–10.5	0.15 ± 0.02	0.03	6.5
d1221+2814	416	5.7	1.0	–11.1	0.05 ± 0.03	0.04	1.3
d1233+3806	740	10.1	1.5	–12.6	0.14 ± 0.02	0.15	0.93
KKSG29	562	7.7	2.5	–13.0	0.14 ± 0.02	0.23	0.61
d1243+2956	1128	15.4	2.7	–13.5	0.56 ± 0.08	0.36	1.56
d1243+4127	444	6.1	2.5	–11.8	0.10 ± 0.01	0.08	1.31
BTS157	644	8.8	1.8	–12.3	0.09 ± 0.02	0.12	0.75
d1312+4147	519	7.1	2.5	–12.9	0.18 ± 0.07	0.21	0.86

name in Col. 1, the heliocentric velocity (Table 1, Col. 9) has been reduced to the motion of the Local Group (Karachentsev & Makarov 1996) V_{LG} (Col. 2). The distances in Col. 3 were derived by assuming a Hubble constant $H_0 = 73$ km s^{-1} Mpc^{-1} (Spergel et al. 2007). Optical diameters in the Holmberg system (Table 1, Col. 3) have been corrected for both absorption and inclination, where the inclination was derived from the axial ratio assuming an intrinsic axial ratio of 0.2 (e.g., Tully 1985, in view of the uncertainties in these inclinations, we did not apply corrections for the possible type dependence of the intrinsic axial ratio):

$$\log a_0 = \log\, a + 0.09\, A_b - 0.2\, \log(a/b),$$

where the foreground absorption in the blue A_b is from Schlegel et al. (1998) (as given in the NED).

The linear diameter $A_{0,i}$ [kpc] follows in Col. 4, the absolute magnitude $M^{0,i}_{b,t}$ corrected for Galactic extinction (Schlegel et al. 1998) in Col. 5. For dwarf galaxies, no internal absorption is assumed.

The total H I mass (Col. 6) was calculated using

$$M_{HI} = 2.355 \times 10^5\, D^2 \int S_v \mathrm{d}v,$$

where D is the distance in Mpc and $\int S_v \mathrm{d}v$ is the integrated HI-flux in Jy km s^{-1}.

The total blue luminosity (L_B) is given in Col. 7. The HI mass-to-luminosity ratio M_{HI}/L_B follows in Col. 8 .

For most of the detected galaxies, the error in the HI-mass is of the order of between 10 to 20%. The uncertainty of ~0.5 mag for the absolute magnitude yields an error in the luminosity of about 50% or more. Hence this is the primary source of error in the M_{HI}/L_B ratio.

In Table 3, we present the non-detected galaxies of our observing run: the galaxy name (Col. 1) is followed by its position (Col. 2), the optical size in arcmin (Col. 3), the morphological type (Col. 4), the group membership suggested by its position (Col. 5), the radial velocity $v_{central}$ used for the center of the observed velocity band (Col. 6) and the rms noise of the observed spectrum in mJy (Col. 7).

3. Discussion and conclusions

A representative sample of about 380 nearby dwarf galaxies with distances $D \leq 10$ Mpc has been discussed by us as part of the Catalogue of Neighbouring Galaxies (CNG Karachentsev et al. 2004). About 75% of these nearby dwarfs were detected in the 21 cm line of neutral hydrogen yielding a median HI-mass to-blue-luminosity ratio ~0.8 in solar units (see Figs. 8 and 10b in CNG). Therefore, many nearby dwarf galaxies have a large amount of gas for further star formation. Huchtmeier & Seiradakis (1985), Carignan & Beaulieu (1989), Begum et al. (2005), and Warren et al. (2007) noted that some nearby dwarf systems, such as DDO154, ESO 215-09, and NGC 3741 have $M_{\rm HI}/L_{\rm B} \sim 10$ in solar units, and HI envelopes of 4 to 7 optical diameters. The CNG sample contains 8 very gas-rich dwarf galaxies with $M_{\rm HI}/L_{\rm B}$ greater than 5 in solar units. Some more extremely gas-rich galaxies were found by Karachentsev et al. (2008) among new optical counterparts of HIPASS sources.

All detected sources in our present paper are gas-rich dwarfs with $M_{\rm HI}/L_{\rm B}$ in the range 0.6 to 6.5 in solar units with a median value of $M_{\rm HI}/L_{\rm B} = 1.1$, almost the same as for the CNG sample. Among them, the dwarf galaxy d1217+4703 can be assigned to the most HI-rich galaxies. It resides in the same scattered Canes Venatici I cloud as three other known gas-rich galaxies: DDO 154, NGC 3741, and UGCA 292.

The sample of 17 detected objects are dwarf galaxies with absolute magnitudes in the range –10.5 to –14.1 with a medium of –12.7. Their linear diameters in the range 0.6 to 3.5 kpc (median: 2.5 kpc) are also typical of nearby dwarf galaxies. Based on the data given in Tables 1 to 3, we recognize that all our dwarf galaxies (apart from the probable background object d0946+6842) can be classified as true companions of the center galaxy of the corresponding groups. The mean radial velocity difference between dwarf companions and the center galaxies is -9 ± 45 km s^{-1}, and its mean rms value $\sigma = 169$ km s^{-1} corresponds to the typical radial velocity dispersion in small galaxy groups.

Finally we should note that the HI detection rate for the present sample of 24% is two times lower than for our previous HI survey of nearby dwarfs (Huchtmeier et al. 2000, 2001). The low detection rate is caused by a few obvious reasons:

a) reduced radio flux caused by the greater distances of the galaxies;
b) increased confusion by neighbouring galaxies caused by smaller angular separations between group members at greater distances;
c) increased radio frequency interferences (RFI) within the protected frequency band at 21-cm wavelength.

Future HI-surveys of new dwarf galaxies within more distant groups should attempt to aquire data of yet higher angular resolution.

Acknowledgements. Based on observations with the 100-m radio telescope of the MPIfR (Max-Planck-Institut für Radioastronomie) at Effelsberg. This project has been partially supported by Deutsche Forschungsgemeinschaft under project-number 436RUS113/900/0-1. We have made extensive use of the NASA/IPAC Extragalactic Database (NED, which is operated by the Jet Propulsion Laboratory, Caltech, under contract with the National Aeronautics and Space Administration), and the Digitized Sky Survey (DSS–1) produced at the Space Telescope Science Institute under US Government grant NAG W–2166.

References

Begum, A., Chengular, J. N., & Karachentsev, I. D. 2005, A&A 433, L1
Carignan, C., & Beaulieu, S. 1989, ApJ, 347, 760
Chiboucas, K., Karachentsev, I. D., & Tully, R. B. 2009, AJ, 137, 3009
Ferrarese, L., Ford, H. C., & Huchra, J. 2000, ApJS, 128, 431
Huchtmeier, W. K., & Seiradakis, J. H. 1985, A&A, 143, 216
Huchtmeier, W. K., Karachentsev, I. D., Karachentseva, V. E., et al. 2000, A&AS, 141, 469
Huchtmeier, W. K., Karachentsev, I. D., & Karachentseva, V. E. 2001, A&A, 377, 811
Huchtmeier, W. K., Krishna, G., & Petrosian, A. 2005 , A&A, 434, 887
Karachentsev, I. D., & Karachentseva, V. E. 2004, Astron. Rep., 48, 267
Karachentsev, I. D., & Makarov, D. I. 1996, AJ, 111, 535
Karachentsev, I. D., Karachentseva, V. E., Huchtmeier, W. K., et al. 2004, AJ, 127, 2031
Karachentsev, I. D., Karachentseva, V. E., & Huchtmeier, W. K. 2007, Astron. Lett., 33, 512
Karachentsev, I. D., Makarov, D. I., & Karachentseva, V. E. 2008, Astron. Lett., 34, 832
Kovac, K., Oosterloo,T. A., & van der Hulst, J. M. 2009 [arXiv:0904.2775]
Ott, M. A., Witzel, A., Quirrenbach, A., et al. 1994, A&A, 284, 331
Sharina, M. E., Karachentsev, I. D., Dolphin, A. E., et al. 2008, MNRAS, 384, 1544
Schlegel, D. J., Finkbeiner, D. P., & Davies, M. 1998, ApJ, 500, 525
Schneider, S. E., Helou, G., Salpeter, E. E., et al. 1983, ApJ, 273, L1
Schneider, S. E., Thuan, T. X., Magri, C., et al. 1990, ApJS, 72, 245
Spergel, D. N., Bean, R., Dore, O., et al. 2007. ApJS, 170, 377
Stierwalt, S., Haynes, M. P., Giovanelli, R., et al. 2009, AJ, submitted
Tifft, W. G., & Huchtmeier, W. K. 1990, A&AS, 84, 47
Tully, R. B. 1985, Nearby Galaxies Catalog (Cambridge: Cambridge University Press)
Warren, B. E., Jerjen, H., & Koribalski, B. S. 2007, AJ, 134, 1849

4. Appendix

Around the position of each galaxy in our sample, we examined a region of 9.3 arcmin radius (i.e., twice the half-power beam width of the Effelsberg telescope) using the Digital Sky Survey (DSS), as well as the velocity and other data provided in the NED. Based on this, if we failed to identify one or more likely sources of confusion with the observed HI profile, we accepted the HI profile to be genuinely associated with the targeted dwarf galaxy.

d0245+3955, d0245+3957, and d0246+3952
These irregular galaxies of low surface brightness form a tight triple sub-system inside the NGC 1023 group.

d0946+6842
This faint object of very low surface brightness was discovered by Chiboucas et al. (2009) as a probable background galaxy behind the M 81 group. There is a strong disagreement between its low luminosity and the broad HI line width, leading to $M_T/L_B \sim 184$[2] and $M_{HI}/L_B = 30$ in solar units. We carefully inspected its surroundings using POSS-II and SDSS and did not find any suitable optical counterpart to explain the detected HI signal. This object would be an interesting target for a more detailed study.

FS 20 = LeG 19 and LeG 18
These dwarf members of the Leo-I group (Karachentsev and Karachentseva 2004) are separated by ~3 arcmin (see Fig. A.1), both being within the antenna beam. LeG 18 was detected within the Arecibo ALFALFA survey as AGC 201970 with $V_{HI} = 636$ km s^{-1}, $W_{50} = 38$ km s^{-1}, and $S = 0.55$ Jy km s^{-1}. FS 20 may be probably identified with AGC 205290 [10 46 42.4 +12 46 58] with $V_{HI} = 915$ km s^{-1}, $W_{50} = 50$ km s^{-1}, and $S = 1.46$ Jy km s^{-1} (Stierwalt et al. 2009). Both objects are within the so-called "Leo HI ring" (Schneider et al. 1983).

CGCG 66-109
This is another dwarf member of the Leo-I group (see Stierwalt et al. 2009), for which $V_{HI} = 777$ km s^{-1}, $W_{50} = 44$ km s^{-1}, and $S = 1.74$ Jy km s^{-1}. Its optical velocity, 982 ± 78 km s^{-1}, from the SDSS DR4 corresponds to a blue knot outside the galaxy centre.

d1150+5546
The marginal narrow HI line ($v = 594 \pm 6$ km s^{-1}) reported by Karachentsev et al. (2007) lies in a radial velocity range with frequent RFI. Therefore, we included this object in Table 3 (upper limits).

d1217+4703 = BTS 109
This is a new tiny member of the Canes Venatici I cloud (see Fig. A.1) with very high HI-mass-to-luminosity ratio of 6.5, and $M_T/L_B = 29$ in solar units.

d1221+2814 = KK 138
Marginal HI detection. The broad HI line width $W_{50} = 186$ km s^{-1} yields an extremely high total-mass-to luminosity ratio of ~250 in solar units.

d1233+3806 = BTS 142
This object was detected also in a blind HI survey at Westerbork (Kovac et al. 2009); $V_{HI} = 719$ km s^{-1}, $W_{50} = 47$ km s^{-1}, and $S = 0.41$ Jy km s^{-1}.

KKSG 29
This is a probable dwarf companion of NGC 4594 (the "Sombrero" galaxy); $V_{LG} = 828$ km s^{-1}. Assuming a distance of 9.33 Mpc (Ferrarese et al. 2000) for NGC4594 the projected separation of KKSG 29 from NGC 4594 is 218 kpc. A difference in radial velocity of 266 km s^{-1} between both galaxies yields an orbital mass estimate of 1.2×10^{13} $M_\odot$ or $M_{orb}/L_B = 140$ in solar units. There are four other probable dwarf companions to the Sombrero galaxy within 200 kpc, KKSG 31, KKSG 32, KKSG 33, and KKSG 34; which are all of type dSphs and not detected in HI.

d1243+2956 = BTS 152
This object is HI-rich, a suitable target for a detailed study in H_α and HI.

d1243+4127
A new dwarf member of the CVn I cloud. It was also detected by Kovac et al. (2009) with $V_{LG} = 436$ km s^{-1}.

d1312+4147 = KKH 82 = UGCA 337
A new member of the CVn I cloud. Its optical velocity of 529 ± 40 km s^{-1} (SDSS DR4) agrees well with the HI velocity. However, the broad HI line width of 234 km s^{-1} yields an extremely high $M_T/L_B = 182$ in solar units. No suitable object for confusion could be found within the antenna beam.

[2] The total mass M_T was calculated by assuming that $\log(M_T/M_\odot) = 2\log(W_{50}) + \log(a) + \log(D) + 3.92$, where the line width W_{50} is in km s^{-1}, the angular diameter (a) is in arcmin and the distance D is in Mpc. Any correction for inclination was neglected because of the high uncertainty in this quantity for irregular galaxies.

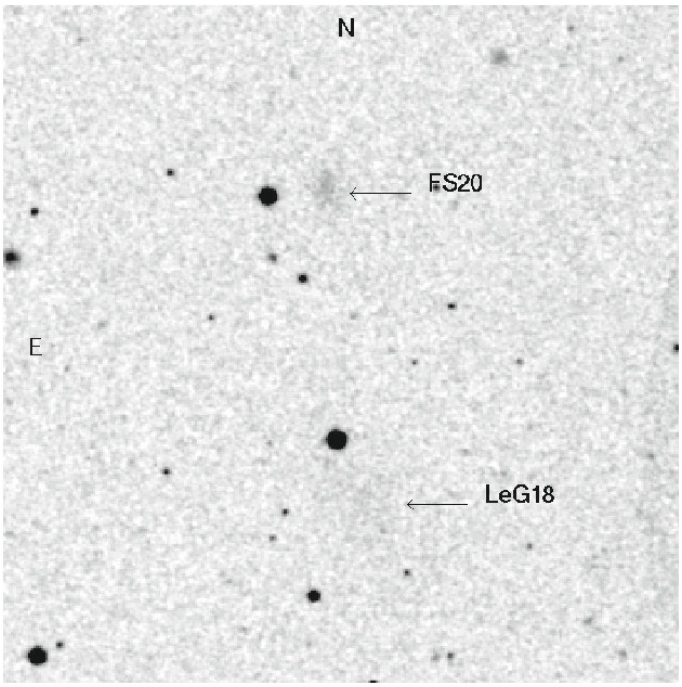

Fig. A. 1 a)

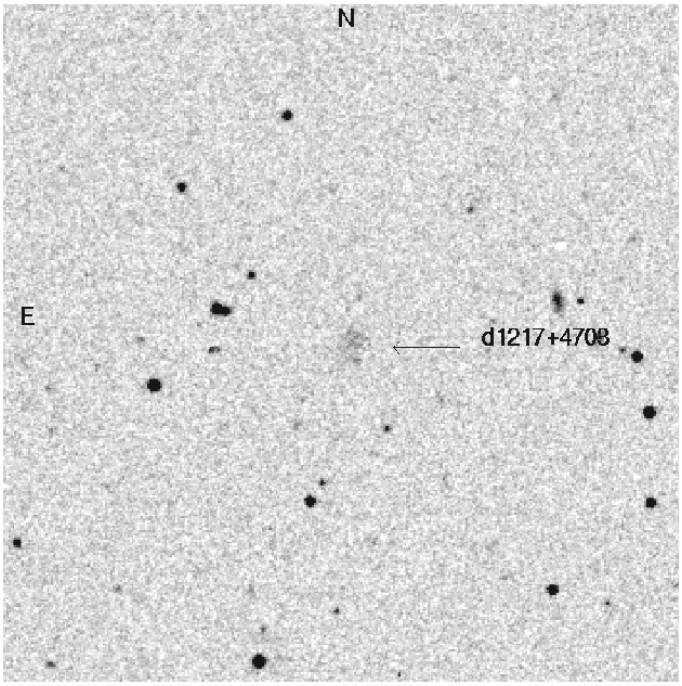

Fig. A. 1 b) Reproductions of the blue POSS-II survey measure 6′ by 6′, north is at top, east at left. The dwarf galaxies FS20 and LeG18 are given in the *upper image* **a)**, while d1217+4708 is shown in the *lower picture* **b)**.

Table 3. Observational data – upper limits.

galaxy name	RA, Dec (2000) h m s ^{o} arcmin $''$	Optical size [arcmin]	Type	Group	$v_{\rm central}$ [km s^{-1}]	rms noise [mJy]
d0224+4102	02 24 20.7 +41 02 12	0.50 × 0.30	Ir	N1023	650	3
d0237+4136	02 37 18.8 +41 36 07	0.40 × 0.35	Ir	N1023	650	3
d0241+3653	02 41 31.5 +36 52 27	0.70 × 0.40	Ir	N1023	650	3
d0243+3759	02 43 02.0 +37 59 26	0.60 × 0.50	Sph	N1023	650	3
d0246+3910	02 46 12.4 +39 10 55	0.75 × 0.50	Ir	N1023	650	3
d0246+3249	02 46 21.8 +32 49 45	0.65 × 0.35	Ir	N1023	650	3
d0246+3832	02 46 49.0 +38 32 51	0.40 × 0.25	Ir	N1023	650	3
d0921+5016	09 21 57.1 +50 16 12	1.10 × 0.90	Sph	N2841	650	4
d0926+7030	09 26 27.9 +70 30 24	0.40 × 0.40	Ir	M81	10	8
d1014+6845	10 14 55.8 +68 45 27	0.20 × 0.20	Ir	M81	10	6
d1018+4109	10 18 22.6 +41 09 58	0.60 × 0.40	Ir	N3180	570	3
d1028+7014	10 28 39.7 +70 14 01	0.70 × 0.45	Sm	M81	10	7
LeG10	10 43 55.4 +12 08 07	0.15 × 0.15	Ir	Leo I	700	5
LeG11	10 44 02.1 +15 35 20	0.50 × 0.45	Ir	Leo I	700	6
FS14, KK93	10 46 24.8 +14 01 30	0.69 × 0.55	Ir	Leo I	700	8
FS40, LeG19	10 49 37.1 +11 21 06	0.60 × 0.40	Ir	Leo I	700	7
UGC 5944	10 50 19.1 +13 16 19	1.10 × 1.05	Sm	Leo I	700	6
LeG28	10 53 00.7 +10 22 45	0.60 × 0.30	Ir	Leo I	700	5
d1058+2006	10 58 16.0 +20 06 26	0.70 × 0.50	Ir	N3507	980	2
LeG33	11 00 45.2 +14 10 20	0.55 × 0.30	Ir	Leo I	700	5
d1106+1250	11 06 10.5 +12 50 42	0.50 × 0.25	Ir	N3507	980	3
d1120+1332	11 20 16.1 +13 32 49	0.60 × 0.35	Ir	N3627	790	4
d1121+1830	11 21 53.8 +18 30 08	0.35 × 0.30	Ir	N3607	900	4
d1129+4606	11 29 25.0 +46 06 47	0.70 × 0.45	Ir	N3726	870	4
d1134+1709	11 34 16.2 +17 09 46	0.70 × 0.40	Sm	N3686	1150	4
d1140+4628	11 40 03.7 +46 28 42	0.60 × 0.50	Sph	N3726	780	5
d1142+5210	11 42 30.1 +52 10 36	0.30 × 0.25	Ir?	N3953	1050	5
d1148+5555	11 48 43.8 +55 55 45	0.60 × 0.45	Ir	N3953	1050	3
d1150+5546	11 50 06.3 +55 46 57	1.00 × 0.70	Ir	N3953	1050	3
d1154+3635	11 54 23.9 +36 35 04	0.70 × 0.60	Ir	N4062	780	3
d1156+5548	11 56 01.2 +55 48 46	0.45 × 0.30	Ir	N3953	1050	4
d1205+4342	12 05 25.0 +43 42 27	0.80 × 0.50	Ir	N4183	930	2
d1212+4237	12 12 18.0 +42 37 32	0.50 × 0.45	Ir	N4183	930	2
d1214+2749	12 14 42.3 +27 49 55	0.35 × 0.30	Ir	N4274	930	4
d1216+3353	12 16 28.8 +33 53 08	0.60 × 0.45	Ir	N4244	250	4
d1216+2928	12 16 39.2 +29 28 46	0.30 × 0.25	Ir	N4274	930	4
d1217+2914	12 17 47.2 +29 14 36	0.40 × 0.40	Ir	N4274	930	5
d1218+2838	12 18 29.4 +28 38 45	0.80 × 0.70	Ir	N4274	930	4
d1218+3003	12 18 31.8 +30 03 36	0.70 × 0.35	Ir	N4274	930	4
d1218+2938	12 18 43.6 +29 38 04	0.40 × 0.35	Ir	N4274	930	4
d1219+4743	12 19 06.5 +47 43 51	0.60 × 0.50	Ir	N4258	450	6
d1220+4700	12 20 40.6 +47 00 03	0.30 × 0.30	dE	N4258	450	6
d1221+2905	12 21 45.8 +29 05 02	0.35 × 0.30	Ir?	N4178	400	4
d1223+2832	12 23 09.5 +28 32 35	0.30 × 0.30	Ir?	N4278	650	4
d1224+4707	12 24 12.0 +47 07 24	0.40 × 0.35	dE	N4346	770	4
d1228+4358	12 28 44.9 +43 58 18	4.00 × 1.00	Ir	N4490	560	6
d1229+3056	12 29 41.2 +30 56 41	0.40 × 0.30	Ir	N4278	650	3
d1230+3002	12 30 25.8 +30 02 24	0.55 × 0.40	Ir	N4278	650	4
d1317+4423	13 17 19.5 +44 23 48	0.80 × 0.50	Ir	N5194	460	5
UGCA 361	13 32 36.2 +49 49 49	1.20 × 0.65	Ir	N5194	460	3
d1348+4335	13 48 57.6 +43 35 57	0.70 × 0.40	Ir	N5194	460	4
UGC 8882	13 57 14.6 +54 06 03	1.10 × 0.80	Sph	M101	250	8
d1504+5538	15 04 51.2 +55 38 42	0.35 × 0.30	Ir	N5906	670	5
d1508+5515	15 08 32.5 +55 15 48	0.50 × 0.40	Ir	N5906	670	5